American Mineralogist, Volume 62, pages 1144–1157, 1977

Channel constituents in cordierite

DON S. GOLDMAN,[1] GEORGE R. ROSSMAN

Division of Geological and Planetary Sciences[2]
California Institute of Technology
Pasadena, California 91125

AND WAYNE A. DOLLASE

Department of Geology, University of California
Los Angeles, California 90024

Abstract

Chemical, optical and infrared absorption, Mössbauer and X-ray data are reported for eight cordierite samples. Fe^{2+} in the octahedral and channel sites is identified in optical and Mössbauer spectra, which indicate that generally less than 5 percent of the total iron is Fe^{2+} in the channels. The single-crystal Mössbauer data of Duncan and Johnston (1974) are reinterpreted. Two types of H_2O are identified and are found to be oriented in the (100) plane with their H–H directions parallel to [001] (Type I) and [010] (Type II). Type II H_2O is found to correlate to the amount of cations in the channels. Optical spectra provide a measure of the hexagonality of cordierite, but these measurements are not correlated with the distortion index, Δ. The color and pleochroism are suggested to arise from intervalence charge-transfer between octahedral Fe^{2+} and channel Fe^{3+}. The strong enhancement of intervalence intensity after dehydration is interpreted in terms of migration of Fe^{3+} from the six-membered tetrahedral rings to the walls of the channel cavities. It is proposed that migration of cations, mainly Na^+, from the rings into the cavities is primarily responsible for changes in the distortion index which accompany dehydration. Values of ϵ (molar absorptivity) for the H_2O absorption bands are determined.

Introduction

The structure of cordierite, $(Mg,Fe)_2Al_4Si_5O_{18}$, consists of six-membered rings of corner-shared Si and Al tetrahedra linked by additional tetrahedra and octahedra. The stacking of the rings forms large cavities parallel to [001] (Gibbs, 1966). Ionic and molecular species such as water, carbon dioxide, argon, helium, and alkaline earth and alkali metal ions have been found in the cavities (Cohen *et al.*, 1977, and others).

In a recent Mössbauer study, Duncan and Johnston (1974) concluded that Fe^{2+} also occurs in the channel cavities. Optical absorption spectra should also indicate the occurrence of Fe^{2+} in multiple sites. However, the optical spectra of cordierite have previously been interpreted only in terms of Fe^{2+} in the octahedral site (Farrell and Newnham, 1967; Faye *et al.*, 1968; Faye, 1972; Smith and Strens, 1976).[3] This discrepancy between the Mössbauer and optical interpretations of cordierite has not been explained.

This paper reports the findings of a combined optical absorption, Mössbauer and X-ray study of eight cordierite samples to (1) identify octahedral and channel Fe^{2+} in optical and Mössbauer spectra, (2) determine the site distribution of iron, (3) reinterpret the single-crystal Mössbauer data of Duncan and Johnston (1974), (4) identify two types of water in the channels and determine their orientation, (5) evaluate the effect of structural state upon the optical spectra, and (6) examine the origin of color and pleochroism.

[1] Present address: Technical Center, Owens-Corning Fiberglas Corporation, Granville, Ohio 43023.

[2] Contribution No. 2843

[3] We refer to the six-coordinate metal site described by Gibbs (1966) as the "octahedral" site to distinguish it from the "channel" site. This does not preclude the possibility of six-coordination for the channel site.

Experimental methods

Single slabs of cordierite were cut and polished using conoscopic interference figures for orientation. The optic orientation for cordierite given in Strunz *et al.* (1971) is $a(\sim 17A) = \gamma$, $b(\sim 9.7A) = \beta$, and $c(\sim 9.3A) = \alpha$. Thicknesses for the optical slabs were determined with a micrometer, and the thicknesses for the slabs used for infrared spectra were also checked by band-intensity ratios and by propping them on their edges, placing them next to a standard of known thickness, and measuring their thickness in a scanning electron microscope. Data reduction for both the optical and Mössbauer spectra have been described previously (Rossman, 1975b; Goldman and Rossman, 1977a). Heating experiments were conducted in air at 200, 500, 800, 900, 1150, and 1250°C for 15.0, 16.3, 6.3, 0.5, 1.0, and 2.0 hours, respectively. Heating experiments on other slabs of different thicknesses produced nearly identical results. Densities for some samples in Table 1 were calculated from the following:

$$\rho(\mathrm{g/cm^3}) = 0.00036[X]^2 + 0.00394[X] + 2.572$$

which is a least-squares solution to the data for 45 samples in Leake (1960) and Strunz *et al.* where $X = (FeO + Fe_2O_3)$ in weight percent.

The Mössbauer spectra of single (001) slabs of samples 3 (1.128 mm thick) and 8 (0.180 mm thick) were obtained on a constant acceleration spectrometer with a Kankeleit-type drive system in which the velocity increment was approximately 0.03 mm/sec/ch. The results of Duncan and Johnston (1974) indicate that these thicknesses represent ideally thin absorbers. Approximately 1.8×10^6 and 2.3×10^6 counts per channel were collected in the off-resonance region for these two samples, respectively, and nearly 4.3×10^6 counts were collected for the powder spectrum of sample 3. The velocity calibration was determined using laboratory foils, and the spectra and spectral parameters are reported relative to iron metal at room temperature.

The distortion index (Δ) in Table 1 was determined from repeated scans in the 28.5–30.5° 2θ region in X-ray diffractograms of powdered material where $\Delta = \{2\theta_{(131)} + [2\theta_{(421)} + 2\theta_{(511)}]/2\}$. Electron microprobe data for each sample are also tabulated in Table 1. They were obtained on a MAC5-5A3 automated microprobe. Data reduction was performed with the program ULTIMATE (Chodos *et al.*, 1973). Emission spectrograph analyses of samples 2, 5 and 8 indicate less than 0.01 percent boron and beryllium.

Channel Fe^{2+}

Optical spectra assignment

The optical spectra of a low-Fe cordierite (Fig. 1) has absorption bands near 995 nm and 1170 nm in α polarization and 935 nm and 570 nm in β and γ polarizations that were assigned to Fe^{2+} in the octahedral site by Farrell and Newnham (1967). Faye *et al.* (1968) alternatively suggested that the bands near 570 nm, which produce the intense color and pleochroism exhibited by cordierite, originate from intervalence charge-transfer between octahedral Fe^{2+} and tetrahedral Fe^{3+}. Faye (1972) indicated that the barycenter (mean) energy for all bands, approximately 13,000 cm^{-1}, is much larger than expected for the size of the octahedral site. A charge-transfer assignment for the 570 nm band results in a barycenter energy for the remaining bands of about 9800 cm^{-1}, which is in better agreement with spectral data for Fe^{2+} in other sites of this size.

Certain problems remain with the Fe^{2+} assignment because there are too many absorption bands arising from the octahedral site. Only two spin-allowed electronic transitions to the split ${}^5E_g$ states are expected in the near-infrared region. The observation of three bands at 935, 995, and 1170 nm suggests that they originate from more than one source. To test this possibility, the intensity relationships among these bands can be compared to those in an Fe-cordierite (sekaninaite) in Figure 2. It is evident that the two bands in α retain the same intensity relationship between each other, which indicates a common origin. These bands are more intense than the bands in β and γ, contrary to the relationship in Figure 1. Hence, the bands in β and γ originate from a different Fe^{2+} source.

Site assignments for the various absorption bands can be clarified utilizing the stoichiometry of each sample, which suggests that most of the iron is in the octahedral site (Table 1). Consequently, only the intensities of the bands due to octahedral Fe^{2+} are expected to correlate with the total iron content among these samples. The intensities of the band in α near 1170 nm and those in β and γ near 935 nm are plotted against the total iron concentration in Figure 3. Gaussian analyses of the α envelope were performed on five samples, and the resulting intensities of the two components are also shown. Their nearly linear correlation with the total iron concentration suggests that they are due to Fe^{2+} in the octahedral site. The erratic variation for the bands in β and γ is

Table 1. Cordierite analyses

	1	2	3	4	5	6	7	8
	weight percent of oxides							
SiO_2	50.37	49.70	49.54	49.97	49.38	48.75	48.16	46.41
TiO_2	--	0.04	--	--	.09	--	0.04	--
Al_2O_3	34.24	32.91	33.47	33.03	33.05	30.69	31.77	32.29
MgO	13.72	12.66	12.42	12.06	10.49	8.99	7.19	2.55
FeO	1.03	2.28	2.46	2.99	5.30	7.35	10.13	16.71
MnO	0.05	--	0.06	0.03	0.31	0.49	0.33	0.68
CaO	--	0.03	0.02	0.01	0.01	0.01	0.02	0.03
Na_2O	0.20	0.36	0.22	0.15	0.21	1.53	0.04	0.55
	99.66	98.00	98.78	98.24	98.85	97.82	97.69	99.22
	formula proportions (Σcations-Na-Ca = 11)							
Si	4.94	5.00	4.97	5.02	5.00	5.05	5.04	4.97
Al	3.96	3.90	3.96	3.91	3.94	3.75	3.92	4.07
Ti	--	--	--	--	0.01	--	--	--
Mg	2.01	1.90	1.86	1.81	1.58	1.39	1.12	0.41
Fe^{2+}	0.08	0.19	0.21	0.25	0.45	0.64	0.89	1.49
Mn	--	--	--	--	0.03	0.04	0.03	0.06
Na	0.04	0.07	0.04	0.03	0.04	0.31	0.01	0.11
Σ^+	35.86	36.02	35.94	35.96	36.02	36.16	36.01	36.12
ρ (g/cm^3)	2.570	2.583*	2.584*	2.587*	2.603*	2.665	2.649*	2.738*
Δ ($2\theta°$)†	0.25	0.27	0.24	0.25	0.27	0.12	0.22	0.22
a (Å)	17.079			17.08		17.036		17.20
b (Å)	9.730			9.74		9.758		9.83
c (Å)	9.356			9.38		9.323		9.30
γ/β**	2.31	2.25	2.03	2.05	2.08	2.12	1.73	2.04

1. *White Well, Australia. Occurs in a phlogopite schist near intrusive granite (Pryce, 1973). X-ray and neutron diffraction data are reported in Cohen et al. (1977).*
2. *Tanga area near Umba River, Tanzania. Occurs with mica schists in alluvial deposits.*
3. *Mt. Tsilaizina, Malagasy Republic.*
4. *Malagasy Republic. Additional Mössbauer, X-ray and chemical data are reported in Duncan and Johnston (1974).*
5. *Manitouwadge, Ontario, Canada. Occurs in a garnet-anthophyllite schist (Pye, 1957).*
6. *Haddam, Connecticut, U.S.A. Occurs in a pegmatite in a biotite gneiss (Heinrich, 1950). X-ray diffraction data are from Meagher (1967). This sample contains 0.52 BeO (Newton, 1966) resulting in 0.13 Be formula units.*
7. *Snyder group northwest of the Kiglapait intrusive, Nain, Labrador. Occurs with biotite and andalusite in a contact aureole (Speer, 1975).*
8. *Dolni Bory, Moravia, Czechoslovakia. Occurs in a pegmatite as massive layers separated by mica (anthophyllite). (Heinrich, 1950; Stanek and Miskovsky, 1964). Cell axes are reported in Strunz et al. (1971).*

**Calculated density (see text). †Δ is the distortion index of Miyashiro (1957). **γ/β is the intensity ratio of the channel Fe^{2+} optical absorption bands near 950 nm.*

consistent with variable amounts of Fe^{2+} in a second site.

The shoulders in β and γ near 1250 nm (Fig. 2) are pronounced only in the high-Fe samples. The shoulders are attributed to components of the 1250 nm transition of octahedral Fe^{2+} which is most intense in α.[4] The different γ/β intensity ratios for samples 7 and 8 (Table 1) suggest that a component of the 995 nm α band is present in β and γ. For samples 7 and 8, the intensities of the β and γ bands are corrected for this component using the intensity of the shoulder and the observed intensity relationship for the bands in α (shown in Fig. 3 by the partially-filled triangles and squares, respectively). The resulting γ/β ratios are more consistent with those for other samples.

The second Fe^{2+} site in cordierite could be either a tetrahedral site or a position in the channel. The nearly linear correlation between Guassian intensity of octahedral Fe^{2+} absorption bands in α and the total iron concentration suggests that a small amount of Fe^{2+} in the second site produces the intense bands in β and γ. Hence, the molar absorptivity (ϵ) for Fe^{2+} in this site must be very large, but large ϵ values can represent Fe^{2+} in either tetrahedral sites or large, distorted sites. Goldman and Rossman (1977b) in-

[4] There is a regular decrease in the energies of the octahedral Fe^{2+} bands as the total iron concentration increases (Fig. 3). This result is consistent with the octahedral site becoming larger as it accommodates more Fe^{2+}.

dicated that Fe^{2+} in large, distorted sites produces absorption bands in both the 1000 and 2000 nm regions. Bands in the 2000 nm region are less intense and are polarized in a different direction from the band near 1000 nm. The band near 2230 nm in α (Figs. 1 and 2) has these characteristics, and probably represents the electronic transition to the remaining ${}^5E_g$ component of Fe^{2+} in the second site. The excellent correlation between this band and those in β and γ (Fig. 4) supports their assignment to the second site. Note that the corrected bands in β and γ for samples 7 and 8 fall on the respective trends. The observation that the bands near 950 and 2230 nm are both produced by Fe^{2+} in the second site suggests that the second site is a position in the channel. Fe^{2+} in a tetrahedral site is not expected to produce absorption bands at wavelengths below about 1500 nm. The crystal-field splitting of E_g state for channel Fe^{2+} is about 6200 cm^{-1}, which is nearly three times the splitting observed for octahedral Fe^{2+} in cordierite. The barycenter energy for channel Fe^{2+} ($\sim$ 7200 cm^{-1}) suggests an average metal–oxygen bond distance of 2.26 A for the coordination site from Faye's (1972, Fig. 3) correlation.

Duncan and Johnston (1974) determined that 20 percent of the total iron content for sample 4 is Fe^{2+} in the channel cavities. However, a significant but variable channel iron content would destroy the linear correlation between the octahedral Fe^{2+} bands and the total iron concentration. To examine the apparent discrepancy between the two spectroscopic techniques, Mössbauer spectra of single crystals of samples 3 and 8 have been obtained to identify channel Fe^{2+} resonance, so that the peak locations can be used to determine the site distribution from the powder spectrum of sample 3.

Site distribution from Mössbauer spectra

Mössbauer spectra of (001) slabs of samples 8 and 3 are presented in Figure 5. The spectrum of sample 4 with this orientation appears in Duncan and Johnston (1974, Fig. 3). The shoulder near 2.0 mm/sec is pronounced only in low-Fe samples, suggesting that it is due to channel Fe^{2+}, because the channel: octahedral Fe^{2+} ratio is more favorable in these samples. The smaller quadrupole splitting suggested from the Mössbauer spectra is consistent for Fe^{2+} in a distorted channel site. Heating experiments also support this assignment. Duncan and Johnston found that as (001) slabs were heated in air to temperatures up to 1380°C, Fe^{3+} resonance appeared in the low-velocity region with a concomitant disappearance of the

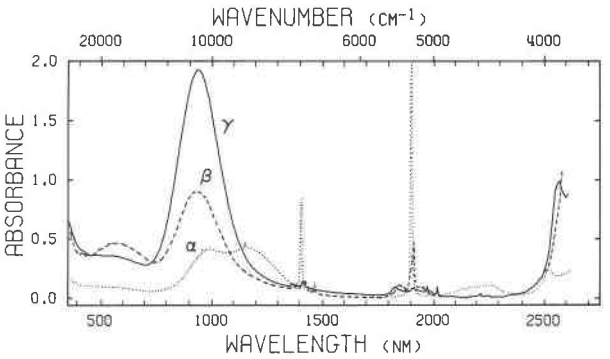

Fig. 1. Room-temperature optical spectra of a low-Fe cordierite from Mt. Tsilaizina (sample 3). Crystal thickness = 1.20 mm.

shoulder near 2.0 mm/sec. Our optical spectroscopic examination of slabs heated in air to similar temperatures indicated that proportionately more channel Fe^{2+} was oxidized. The assignment of the shoulder to Fe^{2+}/Fe^{3+} intervalence charge-transfer by Pollack (1976) is unlikely, because the charge-transfer optical bands near 570 nm increase upon heating. It is also noted that the ratio of intensities of the two components of the octahedral Fe^{2+} resonance at 0.1 and 2.4 mm/sec is the same for the spectra of both the high- and low-iron samples. This indicates that the remaining channel Fe^{2+} peak in the low-velocity region does not have significant intensity.

Single-crystal orientation affects the probability of observing each quadrupole transition differently, but does not affect their energy (Zory, 1965). Therefore, the position of the shoulder can be used as a guideline to analyze the powder spectrum of sample 3 (Fig. 5). The equal intensities of the main peaks indicate a randomly-oriented powder. In fitting the spectrum to two doublets with equal area and halfwidth constraints, the position of the channel Fe^{2+} peak in the

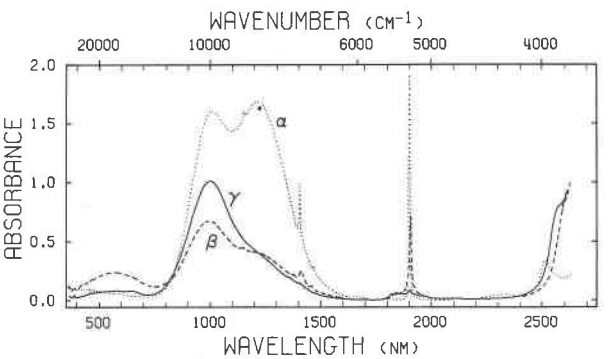

Fig. 2. Room-temperature optical spectra of a high-Fe cordierite from Dolni Bory (sample 8). Crystal thickness = 0.70 mm.

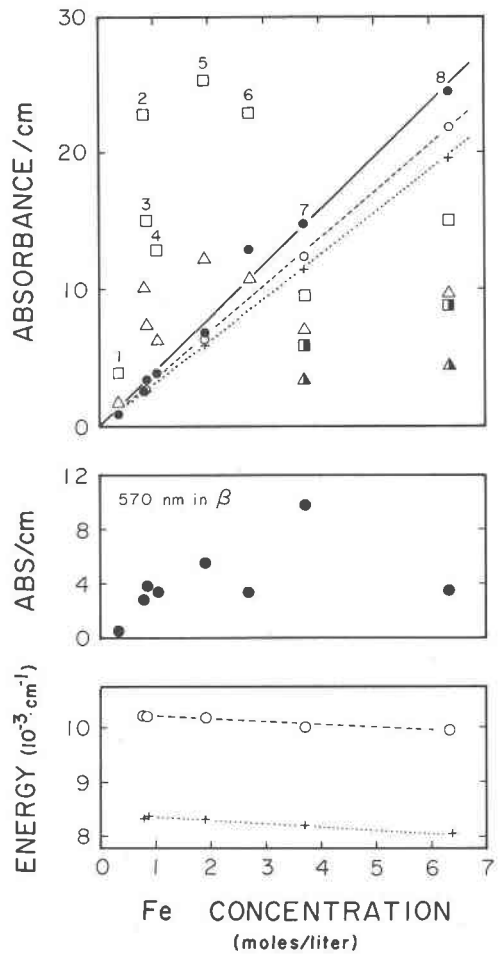

Fig. 3. Upper: Intensity data for the Fe^{2+} absorption bands from optical spectra as a function of the total iron concentration for channel Fe^{2+} near 950 nm in β (△) and γ (□), and octahedral Fe^{2+} near 1170 nm in α (●). Gaussian-fitted intensities to the octahedral Fe^{2+} bands in α near 1000 nm (○) and 1170 nm (+) are also presented. The half-filled squares and triangles are corrections to the intensity of the channel Fe^{2+} bands (see text for explanation).

Middle: Intensity of the intervalence charge-transfer band in β near 570 nm.

Lower: Energies of the octahedral Fe^{2+} absorption bands in α near 1000 nm (○) and 1170 nm (+) from Gaussian fits.

high-velocity region converged to within 0.01 mm/sec of the position determined in the single-crystal spectrum. The resulting octahedral:channel Fe^{2+} ratio of 17:1 is much different than the 4:1 ratio determined for sample 4 by Duncan and Johnston.[5] Samples 3 and 4 have nearly the same total-iron content, but sample 3 has more intense channel Fe^{2+} optical bands, which indicates that the results of Duncan and Johnston are incorrect. They determined the site distribution in Mössbauer spectra of heated powders assuming only channel Fe^{2+} was oxidized. However, optical spectra of slabs heated to similar temperatures demonstrate the partial oxidation of octahedral Fe^{2+}, as will be discussed in a later section.

Duncan and Johnston determined the orientation of the electric field gradient (EFG) for iron in each site. Their computational method depends on an *a priori* knowledge of the correct site distribution, but the results of our study indicate that the site distribution which they used is incorrect. Therefore, their resulting EFG orientations are also incorrect.

The observed intensities of the single-crystal Mössbauer spectra reported by Duncan and Johnston have been reanalyzed. A detailed outline of the model and the calculations is presented in the appendix at the end of the paper. The line intensities calculated from this model agree with those observed by Duncan and Johnston and show significantly better agreement than their calculated values. It should be pointed out that the EFG axes reported by Duncan and Johnston are not orthogonal. The excellent agreement for our model supports the initial interpretation from optical data that essentially all the Fe^{2+} in cordierite is present in the octahedral site. The success of this fit with an EFG axis constrained parallel to [100] further supports the assignment of this iron to the octahedral site.

Water

Orientation

It was suggested from early studies of water in cordierite that it is present as molecular H_2O and as $(OH)_4$ groups replacing some of the tetrahedral SiO_4 groups (Sugiura, 1959; Iiyama, 1960). Subsequently, Schreyer and Yoder (1964) suggested from infrared spectra that molecular H_2O is the sole hydrous component. Later studies confirmed the presence of molecular H_2O and deciphered its orientation in the channel cavities. Farrell and Newnham (1967) and

[5] The resulting parameters from the powder Mössbauer spectrum of sample 3 for quadrupole splitting, isomer shift, and relative area are: (channel Fe^{2+}) 1.60, 1.21 mm/sec, and 5.8 percent; (octahedral Fe^{2+}) 2.31, 1.22 mm/sec, and 94.2 percent. The peak halfwidths are 0.31 mm/sec and χ^2 for 200 channels is 648 with $\sim 4 \times 10^6$ background counts. The presence of Fe^{3+} is suggested in the 0.4–0.5 mm/sec region. Upon removing the equal intensity constraint for the components of the channel Fe^{2+} doublet, the low velocity component became more intense, suggesting additional resonance in this region. However, an Fe^{3+} doublet was not fitted, because its peak positions are not known at 295 K and it accounts at most for only a few percent of the total resonance.

Tsang and Ghose (1972) concluded that the H_2O molecules are oriented in the (100) plane with their H–H direction parallel to [001] based on infrared and nuclear magnetic resonance spectra (NMR), respectively. However, Cohen *et al.* (1977) concluded from a combined X-ray and neutron diffraction study of sample 1, that the H_2O molecules are disordered into four positions with their molecular planes near (001).

Combination and overtone modes of H_2O occur near 1900 and 1400 nm, respectively. An examination of these absorption bands among the eight samples studied revealed two independent sets of bands. One set, referred to as Type I, has absorption bands polarized in α at 1401 and 1898 nm. The other set, referred to as Type II, has absorption bands in β at 1406 and 1903 nm. The distinction between these sets of H_2O absorptions can be best seen in Figure 6. The bands near 1900 nm arise from a combination of the fundamental bending (ν_2) and asymmetric stretching (ν_3) modes, and are polarized in the H–H direction of the H_2O molecule (assuming C_{2v} symmetry). Hence, the two types of H_2O in cordierite are oriented 90° apart with their H–H directions parallel to [001] (Type I) and [010] (Type II). This result is similar to the findings of Wood and Nassau (1967) from the infrared spectra of beryl. Their nomenclature with regard to orientation has been adopted in this study.

The polarization of the combination band near 1900 nm defines the H–H direction of the H_2O molecule, but does not provide information about the orientation of the molecular plane. This information is obtained from the fundamental modes in which ν_1 (symmetric stretch) and ν_2 are polarized along the molecular two-fold rotation axis, and ν_3 is polarized along the H–H direction. Infrared spectra of samples 5 and 6 (Figs. 7 and 8, respectively) show three prominent bands in the fundamental stretching region (3500–3700 cm^{-1}). The greater breadth of the band in β results from a close overlapping of two bands, which are resolved at 78 K. In addition, the intensity

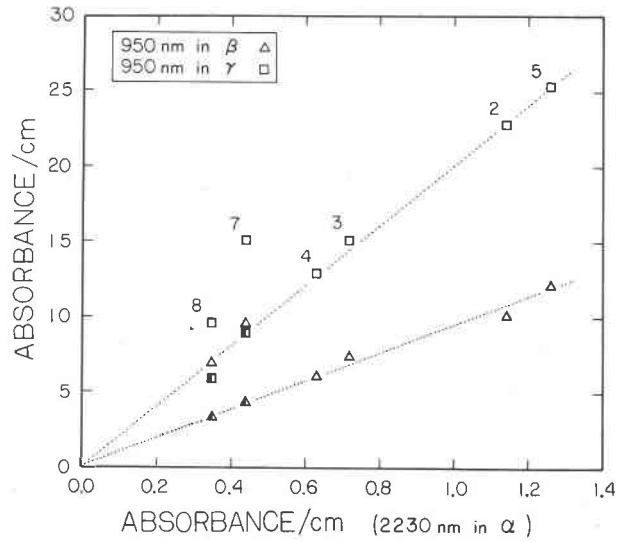

Fig. 4. Correlation of channel Fe^{2+} absorption bands. Symbols are described in Fig. 3.

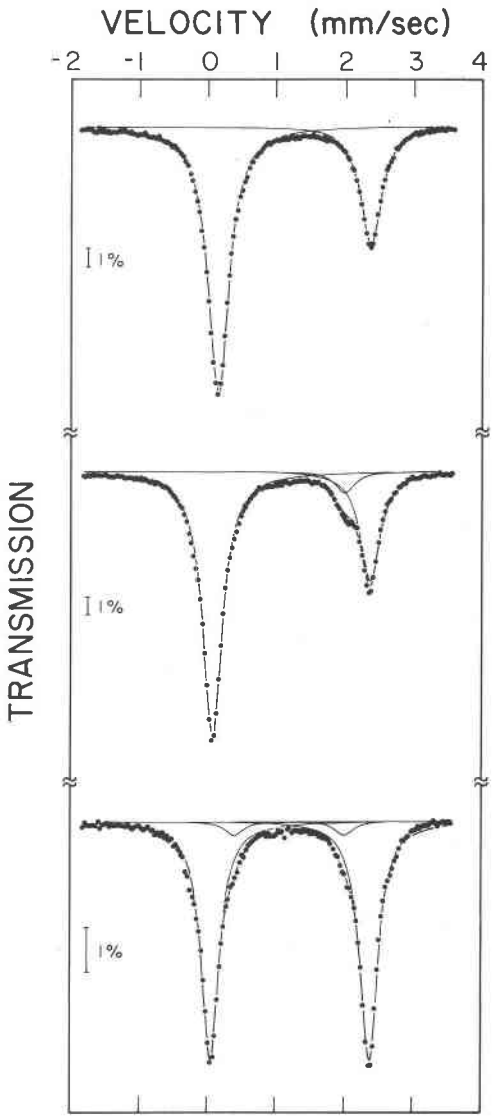

Fig. 5. Upper: Single-crystal Mössbauer spectrum of a high-iron cordierite from Dolni Bory (sample 8) taken at room temperature on a 0.180 mm thick (001) slab.

Middle: Single-crystal Mössbauer spectrum of a low-iron cordierite from Mt. Tsilaizina (sample 3) taken at room temperature on a 1.128 mm thick (001) slab.

Lower: Powder Mössbauer spectrum of a low-iron cordierite from Mt. Tsilaizina (sample 3) taken at room temperature.

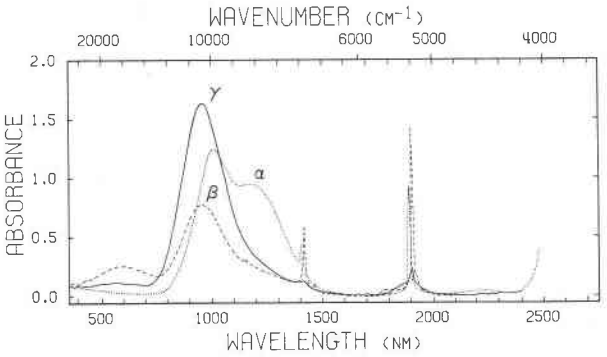

Fig. 6. Room-temperature optical spectra of cordierite from Haddam (sample 6). Crystal thickness = 0.70 mm.

of the band in α at 3689 cm^{-1} correlates with the Type I combination mode at 1898 nm, and the band in α at 3574 cm^{-1} correlates with the Type II combination mode at 1903 nm. The observation of four bands in the fundamental stretching region and their correlation with the combination modes near 1900 nm confirm the presence of two different types of molecular H_2O in cordierite. The polarization of the fundamental stretching modes almost entirely in α and β indicates that the molecular planes of both types of H_2O are parallel to (100). Therefore, they only differ in the orientation of their H–H direction, either parallel (Type I) or perpendicular to (Type II) the channel axis in the (100) plane.

The Type II fundamental modes are obtained using the correlation between the combination mode at 1903 nm and the band at 3574 cm^{-1}, and the intensity relationships among the remaining infrared bands. These correlations indicate that ν_1 and ν_2 occur in α at 3574 and 1630 cm^{-1}, respectively, and ν_3 occurs at

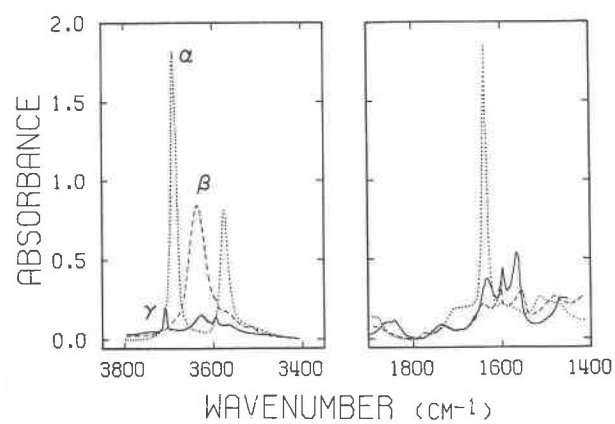

Fig. 7. Room-temperature infrared spectra of cordierite from Manitouwadge (sample 5), showing the fundamental stretching and bending modes of water. Crystal thickness = 0.050 mm.

3632 cm^{-1} in β. The combination mode from $(\nu_2 + \nu_3)$ expected in β at 1900 nm is observed in β at 1903 nm.

The Type I fundamental modes are more difficult to identify. ν_1 and ν_2 are expected in β, and ν_3 is expected in α, based on the complete polarization of the combination mode at 1898 nm in α. ν_3 is easily identified at 3689 cm^{-1} in α, based on its intensity correlation with the combination band. Low-temperature spectra suggest that ν_1 occurs near 3650 cm^{-1} in α and is less intense than ν_3 at 3689 cm^{-1}. The subordinate intensity of ν_1 explains why an excellent correlation exists between the main peak in β (ν_3 of Type II) and ν_1 of Type II H_2O. The fundamental bending mode of Type I H_2O expected in β is also much less intense than ν_3. It is predicted to be at 1580 cm^{-1}, based on the difference between the combination mode $(\nu_2 + \nu_3)$ at 1898 nm (5269 cm^{-1}) and ν_3 at 3689 cm^{-1}. Three features occur in β at 1550, 1600, and 1638 cm^{-1}, which disappear with the other fundamental modes as the sample is dehydrated, also show a correlation with ν_3 of Type I at 3689 cm^{-1}. We do not understand the marked distinction between the two types of H_2O in the fundamental bending region. Nevertheless, the polarization of the fundamental stretching modes and the combination modes near 1900 nm clearly indicate that the molecular plane of each type of H_2O is parallel to (100).

Relationship to other channel constituents

Wood and Nassau (1967) found a correlation between the alkali content and the amount of Type II H_2O in beryl. They proposed that the presence of an alkali ion in the channel reorients an H_2O molecule into a Type II position. A similar correlation is also found in cordierite (Fig. 9), in which the alkali ion is dominantly Na. The unusually high Na content of sample 6 explains the dominance of the Type II H_2O absorption bands in this sample (Fig. 6). The scatter about the alkali trend in Figure 9 is further reduced by accounting for the channel Fe^{2+} content of each sample. The channel Fe^{2+} content for each sample was obtained based on the amount determined from the Mössbauer data of sample 3, the ratio of optical-band intensities for channel Fe^{2+}, and a correction for differences in density. The excellent correlation resulting suggests that the Type II H_2O content is controlled by the positively-charged ions that reside in the channels. Further evidence for this control is suggested from the cordierites studied by Berg and Wheeler (1976). Spectroscopic examination of those samples confirms their suggestion that these cordierites are nearly anhydrous, and their microprobe data

indicate that these samples contain only 0.02 percent Na_2O.

The least-squares solution to the data in Figure 9 is:

$$\text{Abs/cm} = 13.51[\text{CAT}] + 1.58$$

where [CAT] is the concentration (in moles/liter) of Na, Ca, and Fe^{2+} in the channels. The observation that this trend does not intersect the origin suggests that other ions involved in this relationship are present in the channels. The relationship between the *concentration* of Type II H_2O and [CAT] is obtained by dividing the above equation by the ϵ value for this absorption band, which is determined in the next section.

Relative amounts of Type I and Type II H_2O

The relative proportion of each type of H_2O can be determined from infrared spectra once the ϵ values are known. They can be determined from two or more samples, using the absorption-band intensity for each type of H_2O and the total H_2O content. This has been done for the Type I band at 1898 nm in α and the Type II band at 1903 nm in β for samples 1, 3, and 6. The H_2O contents were determined by conventional thermogravimetric analyses of powdered material for sample 1 (G. V. Gibbs, personal communication) and sample 6 (Iiyama, 1960), and by dehydration of a single slab in which weight loss and infrared spectra were sequentially monitored (sample 3, this study). Microprobe analyses of the dehydrated slab of sample 3 did not detect alkali loss. The least-squares solution to this problem, written in matrix notation as

$$\begin{matrix} \text{Absorbance/cm} \\ \text{Type I} \quad \text{Type II} \end{matrix} \qquad \begin{matrix} H_2O \\ \text{(moles/liter)} \end{matrix}$$

$$\begin{bmatrix} 31.36 & 4.04 \\ 21.91 & 3.87 \\ 12.68 & 20.06 \end{bmatrix} \begin{bmatrix} 1/\epsilon_I \\ 1/\epsilon_{II} \end{bmatrix} = \begin{bmatrix} 2.84 \\ 2.31 \\ 3.62 \end{bmatrix}$$

is $\epsilon_I = 13.1$ and $\epsilon_{II} = 7.54$. These results indicate that 84, 77, and 27 percent of the total H_2O content is Type I in samples 1, 3, and 6, respectively. The low proportion of Type II H_2O in most samples is consistent with the NMR results of Tsang and Ghose (1972), who failed to detect Type II H_2O. They studied a sample from the same locality as sample 3. It should be pointed out that these calculations are strongly biased by the accuracy of the data for sample 6. Any loss of CO_2 or other volatiles during dehydration will also affect these results.

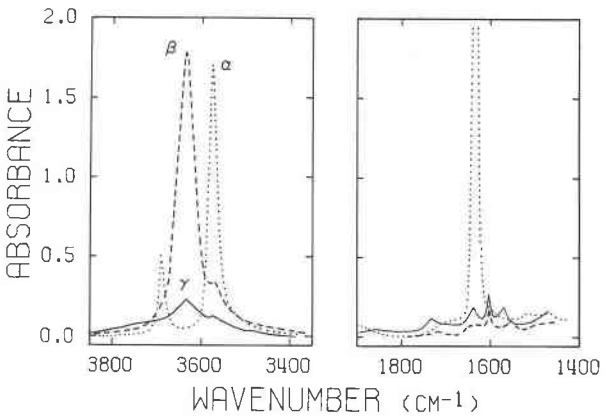

Fig. 8. Room-temperature infrared spectra of cordierite from Haddam (sample 6) showing the fundamental stretching and bending modes of water. Crystal thickness = 0.025 mm.

The least-squares solution to the data in Figure 9 given in the previous section is divided by ϵ_{II} resulting in

$$[C]_{H_2O}^{\text{Type II}} = 1.79[\text{CAT}] + 0.21.$$

The nearly 2:1 ratio between the concentration of Type II H_2O and [CAT] suggests that most of the channel cations, located in or near the center of the six-membered rings (Gibbs, 1966), are additionally coordinated to one Type II H_2O molecule in the cavity above and one in the cavity below the ring. This would result in a more uniform coordination

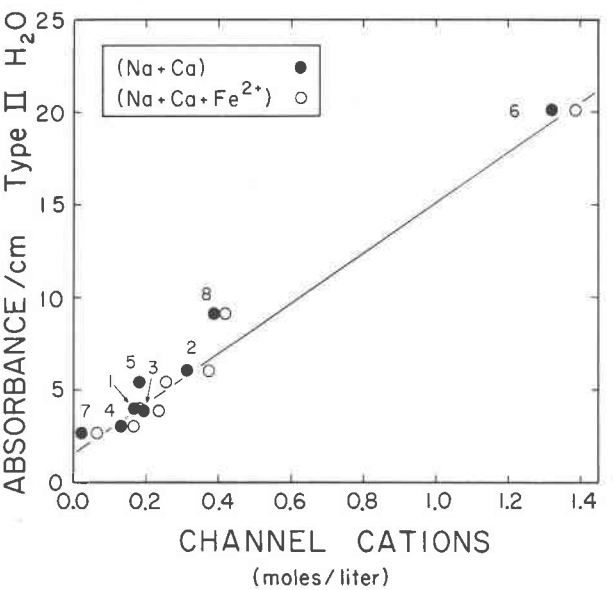

Fig. 9. Correlation of the Type II water band intensity at 1903 nm in β and the amount of Na + Ca (●) and the amount of Na + Ca + Fe^{2+} (○) in the channels in cordierite.

about the channel cation. Assuming a 2:1 ratio, and by accounting for other cations in the channels by moving the least-squares line in Figure 9 to the origin with the same slope, the relative amounts of Type I H_2O in samples 1, 3, and 6 are determined to be 79, 75, and 18 percent, respectively. Hence there is good agreement in calculating the relative proportions of both types of H_2O using the spectral intensities and from an intuitively reasonable coordination relationship between the channel cations and the Type II H_2O.

Structural state

Miyashiro (1957) suggested that cordierite exists in all intermediate structural states between orthorhombic and hexagonal symmetries and attributed the variation to Al/Si ordering in the six-membered rings. Miyashiro defined a distortion index, Δ $\{2\theta_{(131)} - [2\theta_{(421)} + 2\theta_{(511)}]/2\}$, measured from X-ray diffractograms, to represent the deviation from hexagonal symmetry. Later structural refinements (Gibbs, 1966; Meagher, 1967) found the same Si/Al ordering in samples having very different Δ values, which led Stout (1975) to suggest that Δ is also dependent upon compositional factors, such as H_2O in the channels.

Optical spectra must also be sensitive to differences in structural state. In a hexagonal crystal all directions normal to the channel axis are equivalent, and the channel Fe^{2+} bands in β and γ must merge into one band (*i.e.* $\gamma/\beta = 1$). Therefore, γ/β ratios of the channel Fe^{2+} bands from optical spectra also represent deviations from hexagonal symmetry. However, there does not appear to be any correlation between this "optical" hexagonality of cordierite based on the γ/β ratios and the dimensional hexagonality as measured by the Δ index. Therefore, these scales are measuring different phenomena. It must be remembered that Δ (and $a - \sqrt{3}b$) can be equal to zero, in which case the crystal is dimensionally hexagonal but may still possess orthorhombic symmetry.

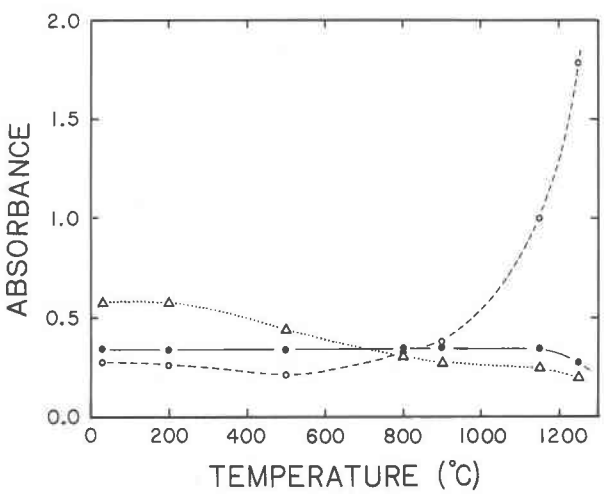

Fig. 10. Results of heating experiments conducted in air on a (100) slab of sample 5. The absorption band intensities for channel Fe^{2+} at 950 nm in β (△), octahedral Fe^{2+} at 1170 nm in α (●), and intervalence charge-transfer at 570 nm in β (○) were monitored after each heating step. Water loss was not detected until 800°C. After 2 hours at 800°C, the sample was completely dehydrated. Crystal thickness represented = 0.5 mm.

Origin of color

Smith and Strens (1976) suggested that the color and pleochroism in cordierite are due to intervalence charge-transfer between Fe^{2+} in the octahedral site and Fe^{3+} in the T_1 tetrahedral site. There are two T_1 sites that each share one edge with the octahedron, such that the metal–metal vectors make angles of 31.5° with [010] in the (001) plane. Three independent observations support this interpretation. First, the structural refinement of Gibbs (1966) indicates that T_1 is an Al-rich tetrahedron, and therefore is a likely site for Fe^{3+}. The presence of Fe^{3+} in this site is consistent with the electron paramagnetic resonance (EPR) data of Hedgecock and Chakravartty (1966). Second, the energy of this charge-transfer band (17,500 cm^{-1}) is significantly higher than most intervalence charge-transfer bands arising from adjacent octahedral sites (Loeffler *et al.*, 1975). Third, components of the charge-transfer process should occur in β and γ, but not in α, as is observed. The observed β:γ intensity ratio of 2.67 is exactly the value predicted using the squares of the direction cosines of the metal–metal vector with [010] and [100]. Despite this strong support for an octahedral–tetrahedral intervalence charge-transfer mechanism, optical spectra taken on slabs of heat-treated cordierite do not support this interpretation.

Sequential heating experiments conducted in air on a (100) slab of sample 5 were performed to monitor changes in the intervalence band intensity, the oxidation of Fe^{2+}, and the loss of H_2O. After heating, samples were cooled to room temperature and spectroscopically examined. The sample was almost totally dehydrated after 2 hours at 800°C. Examination of another slab did not detect H_2O loss up to 775°C. Changes in the intervalence charge-transfer and Fe^{2+} band intensities are summarized in Figure 10. Octahedral and channel Fe^{2+} begin to oxidize above 1150 and 200°C, respectively. The intervalence intensity decreases slightly near 500°C, but continuously increases above 500°C.

Spectroscopic evidence was presented in an earlier

section to suggest that Fe^{2+} occurs in only the octahedral and channel sites. The continuous decrease of the channel Fe^{2+} absorption bands after heating suggests that Fe^{3+} is being produced in the channels. Note that octahedral Fe^{2+} does not begin to oxidize below about 1150°C. Above 500°C, these data suggest that the intervalence charge-transfer in cordierite is due to octahedral Fe^{2+} and channel Fe^{3+}. Support for this interpretation comes from the observation that the same intervalence band at 570 nm increases as more Fe^{3+} is produced in the channels. Furthermore, the same sharp bands of low intensity in the 400–450 nm region, attributed to spin-forbidden transitions of Fe^{3+}, also increase after heating. It is most important to realize that new intervalence and Fe^{3+} absorption bands were not produced after heat treatment. Therefore the observation of the same intervalence and Fe^{3+} bands in all unheated samples indicates that the color and pleochroism in cordierite are due to intervalence charge-transfer between octahedral Fe^{2+} and channel Fe^{3+}.

There is an excellent correlation between the oxidation of Fe^{2+} in the channels and the increase in intervalence charge-transfer intensity only above 800°C, the temperature at which the sample was dehydrated. Below 800°C, the intervalence intensity remained nearly the same. The slight decrease near 500°C may arise from difficulties in accounting for overlapping absorptions on either side of the intervalence band in β polarization. It is proposed that the larger channel cations (Na, Ca, and Fe^{2+}) occur at or near the center of the six-membered rings (Gibbs, 1966) and are coordinated to Type II H_2O molecules, as discussed in a previous section. Smaller cations, such as Fe^{3+}, are probably already present in the channel *cavities,* based on the presence of intervalence bands in all unheated samples. It is reasonable to expect that these ions would situate near the underbonded O_4 and O_5 oxygen atoms that bridge Al- and Si-rich tetrahedra. They would then be in the same (001) plane at $z = 1/4$ as the octahedral sites, and the resulting Fe^{2+}–Fe^{3+} vectors would be similar to those between the octahedral and T_1 sites to produce a similar pleochroism. Most of the Fe^{3+} produced from oxidation by heating remains in the rings, due to the coordination by Type II H_2O. The characteristic absorption-band intensity of Fe^{3+} in the rings is probably low because it is isolated from interacting with Fe^{2+}, and hence is not observed. After dehydration at 800°C, these cations continuously migrate to the walls of the cavities to produce the dramatic increase in the intervalence charge-transfer intensity. There is an indication of electron density loci near the walls of the cavities of sample 1 at fractional coordinates (0.11, 0.16, 0.25) and the symmetry-related positions from room-temperature data (G. V. Gibbs, personal communication). X-ray data for a dehydrated sample, particularly a Na-rich sample, are required to evaluate the model proposed above. Our interpretation does not preclude the presence of tetrahedral Fe^{3+}. It does suggest that any tetrahedral Fe^{3+} present is not dominantly responsible for the color and pleochroism in cordierite.

Discussion

Structural models

Stout (1975, 1976) proposed a model to explain the increase in the distortion index (Δ) that occurs when cordierite powders are heated in air for 2 hours at 900°C. The model attributes the structural readjustment to the loss of H_2O and its influence on the crystal structure from hydrogen bonding to the aluminosilicate framework in the channel cavities. Langer and Schreyer (1976) objected to the influence of H_2O on the crystal structure, pointing out that the infrared frequencies of H_2O in cordierite suggested only weak hydrogen-bonding interactions. Both authors left open the possibility that compositional factors other than Al/Si ordering may be responsible for the observed structural readjustment after heating.

The model proposed in the previous section provides a plausible explanation of Stout's observations, in terms of cation migration from the center of the six-membered tatrahedral rings to the wall of the channel cavities after dehydration. The migration occurs mainly after dehydration, in which the coordinating influence of Type II H_2O with these cations is no longer present. Note that the loss of Na or Fe was not detected from slabs dehydrated at 800°C for 2 hours. Evidence for cation migration after dehydration is based on the rapid increase in intervalence charge-transfer. This increase is interpreted in terms of the oxidation of Fe^{2+} in the rings to Fe^{3+} which migrates to the cavity wall after dehydration. The incorporation of these ions near the cavity wall is a probable mechanism to affect the lattice geometry without invoking an Al/Si redistribution in nearly totally-ordered cordierites.

Quantitative aspects of H_2O

The relative proportions of the two types of H_2O were determined for three samples using their total H_2O content, the spectral intensities of the combination bands, and the suggested 2:1 relationship between Type II H_2O and the channel cations. These

results are used to determine the ϵ values for the fundamental modes of sample 6, which are tabulated in Table 2. Only ν_3 for Type I H_2O was readily observed for a determination of ϵ. It is important to realize that the ϵ values for ν_3 of both types of H_2O are about the same, considering the probable errors in their determination. Consequently, the relative proportion of each type of H_2O can be readily determined from infrared spectra of powdered cordierite.

Yinogradov and Linnell (1971, p. 47) suggested that hydrogen bonding decreases the intensities of overtones. We suggest that this relationship may be used to interpret the intensities of combination bands. For example, the ϵ values of the combination bands of both types of H_2O in cordierite are greater than those of liquid water ($\epsilon \sim 0.9$). An ϵ value of approximately 5 is observed for the combination band in joaquinite (Rossman, 1975a), which is interpreted to have weakly hydrogen-bonded H_2O based on fundamental stretching frequencies.

Quantitative aspects of Fe^{2+}

Goldman and Rossman (1977b) indicated that the ϵ values for Fe^{2+} become greater as the site becomes larger and more distorted. Hence, the ϵ value for channel Fe^{2+} in cordierite is expected to be very large. The Mössbauer data for the powder of sample 3 indicate that 5.8 percent of the total iron is Fe^{2+} in the channels. Using the optical data for this sample (Fig. 1) and this site distribution, an ϵ value of 294 is obtained, the largest ϵ value that we have determined for Fe^{2+}. For comparison, the ϵ values for Fe^{2+} in the highly-distorted grunerite $M4$ site and orthopyroxene $M2$ site are 150 and 40, respectively. The ϵ value for octahedral Fe^{2+} in cordierite is 3.5 for the higher-energy band, and is nearly independent of composition.

Conclusions

(1) Fe^{2+} is present in both the octahedral ($\epsilon \sim 3.5$) and channel ($\epsilon > 200$) sites in cordierite. Channel Fe^{2+} accounts for less than about 5 percent of the total iron content in most samples.

(2) The calculated intensities of the absorption lines in single-crystal Mössbauer spectra better match the observed intensities by assuming that almost all of the iron is present in the octahedral site and by constraining one of the principal EFG axes to coincide with the symmetry axis of the octahedral site.

(3) Two types of molecular H_2O are present in the channels. They are oriented in the (100) plane with their H–H directions parallel to [001] (Type I) and [010] (Type II). Type II is less abundant in most samples and is correlated to the amount of channel cations. We suggest that there are two Type II H_2O molecules, one in the cavity above and one in the cavity below the six-membered tetrahedral ring, that coordinate a cation in the ring.

(4) Optical spectra provide a measure of the hexagonality of cordierite, but a relationship between this "optical" hexagonality and the Δ index was not found.

(5) Color and pleochroism probably arise from intervalence charge-transfer between octahedral Fe^{2+} and channel Fe^{3+}.

(6) We suggest that, after dehydration, the channel cations in the six-membered rings migrate to the wall of the channel cavities.

(7) The ϵ values for the asymmetric stretching mode are nearly the same for both types of H_2O,

Table 2. ϵ values for H_2O in cordierite*

Type	Mode	cm^{-1}	ϵ^a	ϵ^b
I	ν_3	3689	204	308
	$\nu_2 + \nu_3$	5269	13.1**	
II	ν_1	3574	256	228
	ν_2	1630	584	520
	ν_3	3632	269	239
	$\nu_2 + \nu_3$	5255	7.5**	

Spectral data are from sample 6 (Figure 8).
***Determined from a least-squares solution to the data from samples 1, 3 and 6.*
a. Based on the spectral intensity determination from which 27 percent of the total H_2O content is Type I.
b. Based on the assumed 2:1 relationship between Type II H_2O and the channel cation content from which 18 percent of the total H_2O content is Type I.

indicating that their relative proportions can be determined from infrared spectra of powdered samples.

Appendix

Single-crystal Mössbauer analysis

The electric field gradient (EFG) at a particular site within a crystal is a traceless, symmetric, second-order tensor (Zory, 1965). It is described by the magnitudes of the axial components and by their orientation relative to the crystal axes. The principal axes are conventionally chosen so that the magnitudes of the axial components in ascending order are $|V_{xx}| \leq |V_{yy}| \leq |V_{zz}|$ where $(V_{zz} + V_{yy} + V_{xx}) = 0$. Only the relative magnitudes of the axial components are recovered from Mössbauer observations. Therefore, only one variable is needed to describe any inequality among them. This variable is referred to as the asymmetry parameter, η, which is equal to $(V_{xx} - V_{yy})/V_{zz}$. The sign of the EFG is determined by the sign of V_{zz}.

The two absorption lines of a quadrupole split ^{57}Fe doublet represent two separate nuclear transitions ($\pm 3/2 \rightarrow \pm 1/2$ and $\pm 1/2 \rightarrow \pm 1/2$), whose probabilities depend upon the orientation of the gamma-ray beam relative to the EFG at that site. The relative intensities (peak areas) of the two transitions are given by Zory (1965) as $I(3/2) = 4(1 + \eta^2/3)^{1/2} + [3 + \eta)(g\cdot z)^2 + 2\eta(g\cdot x)^2 - \eta - 1]$ and $I(1/2) = 4(1 + \eta^2/3^{1/2} - [(3 + \eta)(g\cdot z)^2 + 2\eta(g\cdot x)^2 - \eta - 1]$, where $(g\cdot x)$ *etc.* are the direction cosines of the gamma-ray beam relative to the EFG axes. A positive value of V_{zz} results in the $\pm 3/2 \rightarrow \pm 1/2$ transition lying at higher energies, while a negative V_{zz} means that the lower energy line represents this transition.

The EFG orientation is given by specifying the orientation of its orthogonal principal axis set (x,y,z) relative to a conveniently-chosen orthogonal reference axis set (a,b,c). For cordierite, the reference axis set may be chosen as coincident with the orthorhombic crystal axes, *a, b, c*. The orientation is specified by the matrix of direction cosines;

$$R = \begin{pmatrix} x\cdot a & x\cdot b & x\cdot c \\ y\cdot a & y\cdot b & y\cdot c \\ z\cdot a & z\cdot b & z\cdot c \end{pmatrix}$$

where $x\cdot a$ is the cosine of the angle between principal axis, *x*, and crystal axis, *a, etc.* The EFG orientations at two different, symmetry-related sites are given by $R' = RS$ where S is the symmetry operation which relates the site at coordinates $u'v'w'$ to the site at coordinates, uvw, such that $[u'v'w'] = [uvw]S$. Only those symmetry operations which produce different EFG orientations need be considered; consequently, translational or inversion components of symmetry operations can be ignored. The result of having several different EFG orientations within a crystal is that the equations giving the intensities of the two transitions will then be a sum of terms, as given above, for each of the EFG orientations present. For iron in the octahedral site in cordierite, there are two EFG orientations related by a two-fold rotation about the crystallographic *c* axis.

At a site within the crystal, the EFG must be invariant to the symmetry of that site, *i.e.* RS must give the same orientation as R for each symmetry element of that site. For example, the octahedral site lies on a two-fold axis which is parallel to [100]. As a result, *one* of the principal axes of the EFG *must* lie along [100]. For analogous cases see *e.g.,* vivianite, (Greenwood and Gibb, 1971, p. 137), FeF_2 (Wertheim, 1961) or sodium nitroprusside (Grant *et al.,* 1969).

A least-squares refinement routine has been programmed to fit the observed Mössbauer intensities to those calculated as a function of the asymmetry parameter, η, and the orientation matrix, R. For this purpose, the terms $(g\cdot x)$ and $(g\cdot z)$ in the intensity equations given above are replaced with expressions involving the orientation matrix, viz;

$$\begin{pmatrix} g\cdot x \\ g\cdot y \\ g\cdot x \end{pmatrix} = R \begin{pmatrix} g\cdot a \\ g\cdot b \\ g\cdot c \end{pmatrix}$$

where the direction cosines of the gamma-ray beam relative to the reference (crystal) axes are known for each Mössbauer spectrum. This refinement procedure has been applied to the fifteen observed intensities reported by Duncan and Johnston (1974). Although they assigned 79 percent of the total iron to the octahedral site and 20 percent to a channel site, we conclude that their cordierite has about 95 percent of the total iron in the octahedral site. Their observations are therefore considered to be due to ^{57}Fe atoms in the set of symmetry-equivalent octahedral sites only, with contributions to the area from channel iron being negligible. A constraint on the refinement of the orientation matrix is that one of the principal axes must parallel [100] (a constraint not applied by Duncan and Johnston). The value of the asymmetry parameter will lie between zero and one when the axes are labeled in ascending order. It is computationally expedient to refine η without constraint on its

Table 3. Comparison of observed and calculated single-crystal Mössbauer spectral intensities

#	g.a[a]	g.b	g.c	OBS[b]	CAL[c]	DIF	CAL(D&J)[d]	DIF(D&J)
1	1.000	0.000	0.000	0.603	0.604	-0.001	0.569	0.034
2	0.891	0.454	0.000	0.602	0.598	0.004	0.588	0.014
3	0.743	0.669	0.000	0.602	0.590	0.011	0.595	0.007
4	0.707	0.000	0.707	0.448	0.463	-0.016	0.457	-0.009
5	0.616	0.788	0.000	0.582	0.585	-0.003	0.592	-0.010
6	0.391	0.921	0.000	0.576	0.578	-0.002	0.590	-0.014
7	0.174	0.985	0.000	0.573	0.574	-0.001	0.582	-0.009
8	0.000	1.000	0.000	0.571	0.573	-0.002	0.573	-0.002
9	0.000	0.966	0.259	0.554	0.556	-0.003	0.559	-0.005
10	0.000	0.866	0.500	0.510	0.510	-0.001	0.517	-0.007
11	0.000	0.500	0.866	0.394	0.385	0.009	0.405	-0.011
12	0.000	0.259	0.966	0.346	0.340	0.007	0.363	-0.017
13	0.000	0.000	1.000	0.310	0.323	-0.012	0.346	-0.036
14	-0.259	0.000	0.966	0.351	0.342	0.009	0.359	-0.008
15	-0.500	0.000	0.866	0.390	0.393	-0.003	0.401	-0.011
						0.007 rms		0.016 rms

a. *direction cosines of gamma-ray beam relative to crystal axes.*
b. *fraction of doublet area represented by higher energy peak, as observed by Duncan & Johnston (1974).*
c. *higher energy peak fraction calculated from model proposed in this study.*
d. *higher energy peak fraction calculated by Duncan & Johnston from their model.*

value and then to rearrange the axial labels to give their conventional order. This procedure eliminates having to refine six models differing in the choice of the sign of V_{zz} and which principal axis is constrained to lie along [100].

The results of the refinement of the Duncan and Johnston observations are summarized in Table 3. The model results in $\eta = 0.16 \pm 0.05$ and V_{zz} being negative. The two symmetry-related orientation matrices are;

$$\begin{pmatrix} 1.0 & 0.0 & 0.0 \\ 0.0 & 0.9044 & -0.4267 \\ 0.0 & 0.4267 & 0.9044 \end{pmatrix}$$

and

$$\begin{pmatrix} 1.0 & 0.0 & 0.0 \\ 0.0 & 0.9044 & 0.4267 \\ 0.0 & 0.4267 & -0.9044 \end{pmatrix}$$

which results in the x principal axis of the EFG lying along [100]. The probable error in orientation of the EFG is about 2°.

Because a small amount of the area of the Mössbauer spectrum is due to Fe^{2+} in a second site, EFG calculations made ignoring this contribution must be somewhat in error. To assess the magnitude of this error, a trial calculation was made as follows. If the EFG orientation (and asymmetry parameter) of the second Fe^{2+} site was the same as that of the octahedral site Fe^{2+}, no error in recovering this orientation from the data would occur. Consequently, a "worst case" EFG orientation (and its symmetry-equivalent orientations) was chosen for the channel site Fe^{2+} which gave, as far as possible, a doublet asymmetry always opposed to that of the octahedral site doublet. Then, assuming the channel site Fe^{2+} contributed 5 percent of the total intensity, its effect was subtracted from the Duncan and Johnston observations. The "corrected" Mössbauer data were then refit by least-squares methods, yielding a negative V_{zz}, $\eta = 0.07$, $V_{xx} = a$ and $z \wedge b = 69°$. The differences between the two sets of results for the octahedral site Fe^{2+}, even assuming the worst orientation of the second site EFG, are small, amounting to only about twice the estimated errors in these parameters.

Acknowledgments

We thank G. V. Gibbs (Virginia Polytechnic Institute and State University), E. P. Meagher (University of British Columbia), R. F. Dymek (California Institute of Technology), J. H. Berg (University of Massachusetts), R. H. Currier (San Marino, California), and J. F. Duncan (Wellington, New Zealand) for supplying many of the samples used in this study. We are especially indebted to R. M. Houseley (Rockwell International) for obtaining the Mössbauer data. In addition, we thank G. V. Gibbs, E. P. Meagher, G. E. Brown (Stanford University), and J. H. Stout (University of Minnesota) for discussing many of the results. This research was supported, in part, by NSF Grants DES 74-19918 and EAR 76-02014.

References

Berg, J. H. and E. P. Wheeler (1976) Osumilite of deep-seated origin in the contact aureole of the anorthositic Nain Complex, Labrador. *Am. Mineral., 61,* 29–37.

Chodos, A. A., A. L. Albee, A. J. Gancarz and J. Laird (1973) Optimization of computer-controlled quantitative analysis of minerals. *Proc., Eighth Natl. Conf. Electron Probe Analysis,* 45A–45C.

Cohen, J. P., F. K. Ross and G. V. Gibbs (1977) An X-ray and neutron diffraction study of hydrous low cordierite. *Am. Mineral., 62,* 67–78.

Duncan, J. F. and J. H. Johnston (1974) Single-crystal ^{57}Fe Mössbauer studies of the site positions in cordierite. *Austr. J. Chem., 27,* 249–258.

Farrell, E. F. and R. E. Newnham (1967) Electronic and vibrational absorption spectra in cordierite. *Am. Mineral., 52,* 380–388.

Faye, G. H. (1972) Relationship between crystal-field splitting parameter, "Δ_{VI}", of absorption spectra of Fe^{2+}-bearing materials. *Can. Mineral., 11,* 473–487.

———, P. G. Manning and E. H. Nickel (1968) The polarized optical absorption spectra of tourmaline, cordierite, chloritoid and vivianite: ferric-ferrous electron interaction as a source of pleochroism. *Am. Mineral., 53,* 1174–1201.

Gibbs, G. V. (1966) The polymorphism in cordierite I: The crystal structure of low cordierite. *Am. Mineral., 51,* 1068–1087.

Goldman, D. S. and G. R. Rossman (1977a) The spectra of iron in orthopyroxene revisited: the splitting of the ground state. *Am. Mineral., 62,* 151–157.

——— and ——— (1977b) The identification of Fe^{2+} in the $M(4)$ site of calcic amphiboles. *Am. Mineral., 62,* 205–216.

Grant, R. W., R. M. Houseley and U. Gonsor (1969) Nuclear field gradient and mean square displacement of the iron sites in sodium nitroprusside. *Phys. Rev., 178,* 523–530.

Greenwood, N. N. and T. C. Gibb (1971) *Mössbauer Spectroscopy.* Chapman and Hall, London.

Hedgecock, N. E. and S. C. Chakravartty (1966) Electron spin resonance of Fe^{3+} in cordierite. *Can. J. Phys., 44,* 2749–2755.

Heinrich, E. W. (1950) Cordierite in pegmatite near Micanite, Colorado. *Am. Mineral., 35,* 173–184.

Iiyama, J. T. (1960) researches sur le rôle de l'eau dans la structure et le polymorphisme de la cordierite. *Bull. Soc. fr. Mineral. Cristallogr., 83,* 155–178.

Langer, K. and W. Schreyer (1976) Apparent effects of molecular water on the lattice geometry of cordierite: a discussion. *Am. Mineral., 61,* 1045–1050.

Leake, B. E. (1960) Compilation of chemical analyses and physical constants of natural cordierites. *Am. Mineral., 45,* 282–298.

Loeffler, B. M., R. G. Burns and J. A. Tossell (1975) Metal-metal charge transfer transitions: Interpretation of visible region of the Moon and lunar materials. *Proc. 6th Lunar Sci. Conf.,* 2663–2676.

Meagher, E. P. (1967) *The Crystal Structure and Polymorphism of Cordierite.* Ph.D. Thesis, The Pennsylvania State University, University Park, PA.

Miyashiro, A. (1957) Cordierite–indialite relations. *Am. J. Sci., 255,* 43–62.

Newton, R. C. (1966) BeO in pegmatitic cordierite. *Mineral. Mag., 35,* 920–927.

Pollack, H. (1976) Charge transfer in cordierite. *Phys. Stat. Solidi, 74,* K31–34.

Pryce, M. W. (1973) Low-iron cordierite in phlogopite schist from White Well, Western Australia. *Mineral. Mag., 39,* 241–243.

Pye, E. G. (1957) Geology of the Manitouwadge area. *Ont. Dept. Mines Rep., 66,* part VIII, 1–114.

Rossman, G. R. (1975a) Joaquinite: the nature of its water content and the question of four-coordinated ferrous iron. *Am. Mineral., 60,* 435–440.

——— (1975b) Spectroscopic and magnetic studies of ferric iron hydroxy sulfates: intensification of color in ferric iron clusters bridged by a single hydroxide ion. *Am. Mineral., 60,* 698–704.

Schreyer, W. and H. S. Yoder (1964) The system Mg–cordierite–H_2O and related rocks. *Neues. Jahrb. Mineral. Abh., 101,* 271–342.

Smith, G. and R. G. J. Strens (1976) Intervalence transfer absorption in some silicate, oxide and phosphate minerals. *In* R. G. J. Strens, Ed., *The Physics and Chemistry of Minerals and Rocks,* p. 583–612. John Wiley and Sons, New York.

Speer, J. A. (1975) The contact metamorphic aureole of the Kiglapait intrusion. *In* S. A. Morse, Ed., *The Nain Anorthosite Project, Labrador: Field Report 1974,* p. 17–26. University of Massachusetts, Amherst, Mass.

Stanek, J. and T. Miskovsky (1964) Iron-rich cordierite from pegmatite near Dolni Bory (in Czech). *Casopis Mineral. Geol., 9,* 191–192.

Stout, J. H. (1975) Apparent effects of molecular water on the lattice geometry of cordierite. *Am. Mineral., 60,* 229–234.

——— (1976) Apparent effects of melecular water on the lattice geometry of cordierite: a reply. *Am. Mineral., 61,* 1041–1044.

Strunz, H., Ch. Tennyson and P. J. Vebel (1971) Cordierite. Morphology, physical properties, structure, inclusions, and oriented intergrowths. *Minerals Science and Engineering, 3,* 3–18.

Sugiura, K. (1959) Water in cordierite. *Tokyo Kogyo Daigaku Gakuho, Ser. B,* No. 1, 26 p.

Tsang, T. and S. Ghose (1972) Nuclear magnetic resonance of ^{1}H and ^{27}Al and Al–Si order in low cordierite, $Mg_2Al_4Si_5O_{18}\cdot nH_2O$. *J. Chem. Phys., 56(7),* 3329–3332.

Wertheim, G. K. (1961) Hyperfine structure of Fe^{57} in paramagnetic and antiferromagnetic FeF_2 from the Mössbauer effect. *Phys. Rev., 121,* 63–66.

Wood, D. L. and K. Nassau (1967) Infrared spectra of foreign molecules in beryl. *J. Chem. Phys., 47,* 2220–2228.

Yinogradov, S. N. and R. H. Linnell (1971) *Spectroscopic Manifestation of Hydrogen Bonding.* Van Nostrand, Reinhold Company, New York.

Zory, P. (1965) Nuclear electric-field gradient determination utilizing the Mössbauer effect (Fe^{57}). *Phys. Rev., 140A,* 1401–1407.

Manuscript received, January 10, 1977; accepted for publication, June 7, 1977.